Why is it so difficult to work on geochemical composition? Supervised geochemical composition data processing to study colouring iron oxide-rich rocks in archaeological contexts

C. Chanteraud, Hélène Salomon, Emilie Chalmin, Quentin Lemasson, Claire Pacheco, Laurent Pichon, Éric Goemaere, Camille Noûs, Brandi Lee Macdonald

Why is it so difficult to work on geochemical composition? Supervised geochemical composition data processing to study colouring iron oxide-rich rocks in archaeological contexts.

Claire Chanteraud[2,1], Hélène Salomon[1], Emilie Chalmin[1], Quentin Lemasson[3], Claire Pacheco[3], Laurent Pichon[3], Eric Goemaere[4], Camille Noûs[5], Brandi L. MacDonald[1]

[1] *Archaeometry Laboratory, University of Missouri Research Reactor, Columbia (MO), USA*

[2] *Environnement DYnamique et territoire de Montagne (EDYTEM), University Savoie Mont Blanc, Chambéry, France*

[3] *Centre of Research and Restoration of French Museum (C2RMF), Paris, France ; Fédération de recherche New AGLAE, FR3506 CNRS/Ministère de la Culture/Chimie Paristech – PSL, Paris, France*

[4] *Geological Survey of Belgium, Royal Belgian Institute of Natural Sciences, Brussels, Belgium*

[5] *Cogitamus Laboratory, 1 ¾ rue Descartes, 75005 Pari, France*

Abstract

Iron oxide-rich colouring materials exhibit substantial diversity across various contexts, encompassing a wide range of physical, chemical, petrographic, and mechanical characteristics. The identification of these materials holds the key to understanding exploited mineral resources and the criteria of selections in Palaeolithic societies. Geochemical methods delve into the intrinsic properties of rocks, offering insights into their historical records, including their formation, weathering transformation, and technical applications. Therefore, for the comprehensive collection and analysis of geochemical data pertaining to such archaeological materials, this paper proposes to establish a foundation with diverse iron oxide-rich reference materials. This serves a triple purpose: 1) formulation of measurement procedures tailored to the unique physical attributes of iron oxide-rich materials, 2) elucidation of the geological formation and context in relation to material composition, and 3) facilitating comparisons between geochemical analyses conducted on archaeological specimens and compatible geological references, whether local, regional, or extra-regional. The aim is to ensure a consistent basis for comparison.

This paper presents a comprehensive investigation of the geochemical composition of seven selected iron oxide-rich reference rocks. The objective is to provide a robust framework for conducting geochemical analyses and statistical data processing on archaeological specimens and relevant reference rocks, leveraging non-invasive Proton-Induced X-ray Spectroscopy (PIXE) data.

Highlights

- Petrographical characterisation of iron oxide-rich rocks
- Geochemical data acquisition by PIXE method
- Statistical data exploration
- Implication on raw colouring material discrimination

Author credits

- Claire Chanteraud: Conceptualisation; investigation; writing - original draft; formal analysis; data curation; visualization
- Hélène Salomon: formal analysis, conceptualisation; writing - review and editing
- Émilie Chalmin: Writing - review and editing; supervision; funding acquisition
- Quentin Lemasson: formal analysis, processing data, review
- Claire Pacheco: formal analysis, review
- Laurent Pichon: formal analysis, processing data, review
- Eric Goemaere: conceptualisation; review and editing
- Camille Noûs: Methodology; conceptualisation; resources; writing - review and editing
- Brandi L. MacDonald: review and editing; supervision; funding acquisition

1. Introduction

Iron oxide-rich colouring materials, discovered in archaeological deposits since the Middle Stone Age in Africa and the Middle Palaeolithic in Europe, also frequently utilized in cave art from the Upper Palaeolithic onwards, hold a central role in the study of prehistoric societies. These materials exhibit remarkable visual, tactile, and mechanical properties, enabling them to be used (e.g., Audoin andPlisson, 1982; Culey et al., 2023; Dayet et al. 2016; Garate et al., 2004; Huntley et al., 2015; MacDonald et al., 2019; Rosso et al. 2016; Salomon et al. 2021; Šajnerová-Dušková et al., 2009; Svoboda, 2008; Velliky et al. 2018 ,). They serve as tangible evidence of the various technical and decorative practices among diverse prehistoric human groups. These materials bear witness to the choices of raw materials made in the past, the locations of their extraction, and the skills and knowledge required to achieve production goals.

To address questions pertaining to the use of these materials, the establishment of geological references becomes a prerequisite to assess the selections and uses of mineral resources by Palaeolithic hunter-gatherer populations. The examination of networks involving colouring materials gains its full significance within the broader context of resource exploitation shells, fauna, flint, and diverse mineral resources.

The trajectories of colouring materials, from their formation to acquisition and transformation, unfolds through the lens of their natural history: genesis, diagenesis, weathering (in line with the "evolutionary chain" concept as proposed by Fernandes, 2012) and cultural ("chaîne opératoire" *sensu* Leroi-Gourhan 1964, Pelegrin 1995), where human-induced transformations come into play. Grinding and mixing with other substances, destroy the petrographic characteristics of the original rock, rendering identification by observation and most analytical methods unfeasible (Salomon et al, 2021).

To describe the selection and procurement of raw colouring materials by Palaeolithic societies, especially when petrographic information is lacking or insufficient, the geochemical approach has gained wide acceptance (Beck et al., 2011; David et al., 1993; Dayet et al. 2022; Eiselt et al., 2012; Green and Watling 2007; MacDonald et al. 2018; Mathis et al., 2014; Mauran et al., 2019; Menu and Walter, 1992; Lebon et al., 2018; Pierce et al. 2020; Popelka-Filcoff et al. 2012; Zipkin et al. 2020). This approach scrutinizes the ability of rocks to retain a chemical signature of their geological origin in their major, minor, and trace element composition (. However, building a geological reference collection is a requirement to gather adequate information about these diverse colouring rocks within a region of study. This diversity encompasses various rock types and lithologies (sedimentary claystone, sandstone, limestone, weathering rocks, hydrothermal mineralization, etc.), mineral compositions (comprising nature, shape, size, abondance, distribution, and chemical composition of minerals), and chemical compositions that span a wide range of iron-oxide content, from 20% to over 95% (as illustrated in Figure 1; Salomon et al., 2021).

Given that archaeological colouring remains are considered vulnerable heritage artifacts, a precise non-invasive approach is essential, and µ-Proton Induced X-ray Spectroscopy (µ-PIXE) stands out as a dependable and efficient technique for determining the geochemical signatures of various material types: obsidian, garnet, variscite, lapis lazuli (Bellot-Gurlet et al., 2005; Calligaro et al., 2002; Lo Giudice et al., 2017; Mathis et al., 2008; Orange et al., 2017; Querré et al., 2008; Querré et al., 2014). In addition, these archaeological colouring materials are often retrieved as small pieces or fragments (under a centimeter size) offering limited analysis areas (< mm²) restricting petrographic identification. Moreover, applied residues and paintings on other substrate materials require analysing strategy of µ-samples that allows their comparison with a diverse reference sample (block and fragment patinated or showing fresh break, powder, thin section, polished section, etc.).

This paper presents a method grounded in a dataset of geochemical information obtained from documented geological collections. The goal is to identify rock type markers (e.g., sedimentary, weathering, hydrothermal) by utilizing geochemical measurements in conjunction with petrographic data from reference samples, in order to identify the provenance of archaeological iron oxide-rich rocks. To ensure the reliability of the geochemical data, analytical conditions were carefully selected to yield pertinent and robust data for subsequent statistical analysis. The resulting statistical chemical space is aligned with the petrographic groupings of reference materials, employing supervised statistical methods. This approach yields valuable insights for comparing reference samples with groups of archaeological artifacts of both unknown geological origin and geographical provenance.

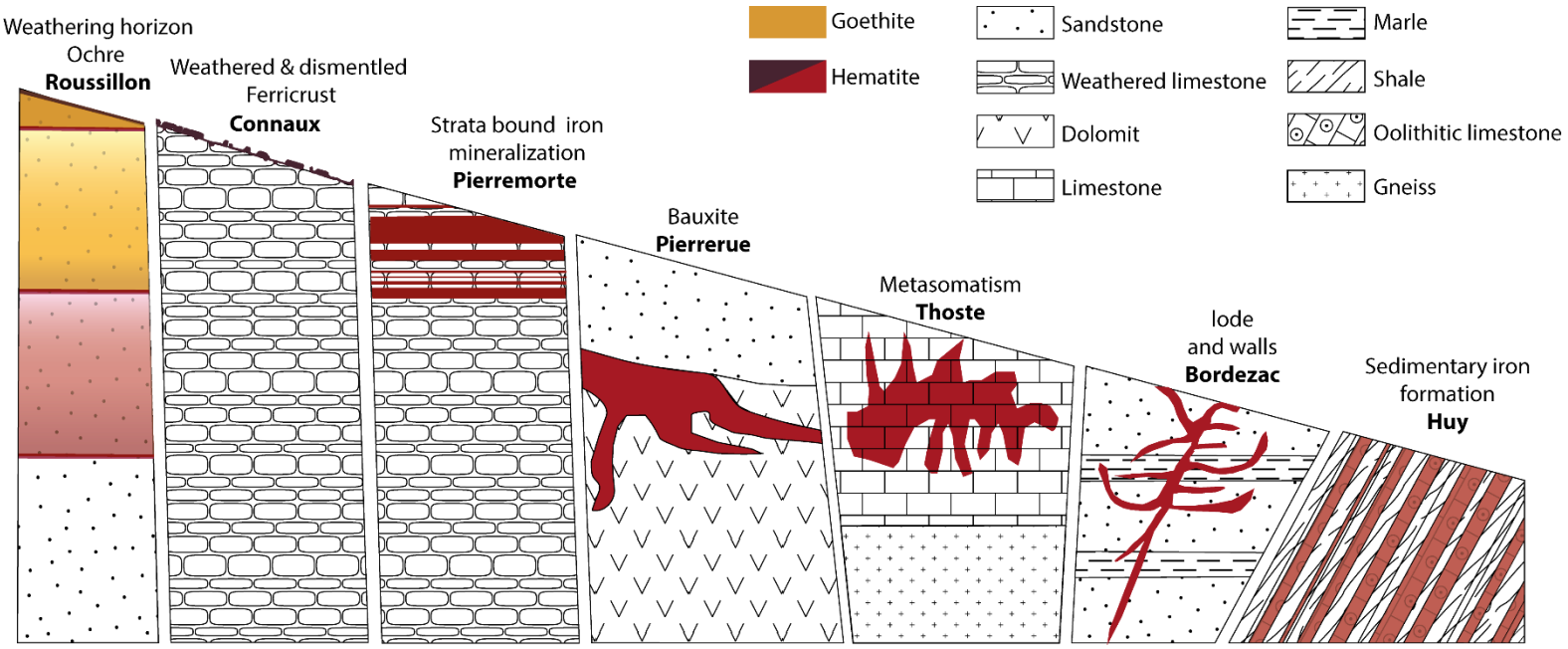

***Figure 1**: Illustration of chosen iron oxide-rich rocks formation as geological references*

2. Material

2.1 Selection of geological references

Seven reference materials were selected from the Pigment Library's collection (Figure 2) to illustrate the diversity of iron oxide-rich rocks and highlight the significant petrographic and geochemical differences among colouring rocks. The selection criteria were based on characteristics such as the type of formation (genesis), petrographic features (structures, grain content, binding phase – matrix and/or

cement), mineralogical assemblage, and their variable iron content (Salomon et al., 2021 ; Chalmin et al. 2020)).

- Hydrothermal hematite mineralization filling a vein in arkosic Triassic sandstone (Bordezac, south-east France). Rare tabular micas (100 µm) and quartz are inherited from the hostrock (mineralogy is described in the SSHADE/PIG (OSUG Data Center) Dataset/Spectral Data. https://doi.org/10.26302/SSHADE/EXPERIMENT_BS_20200422_100).

- Oolitic ironstone (Clinton type) interbedded between Frasnian and Lower Famennian shales (Huy, Wallonia, south-east Belgium). The rock shows well-sorted ferruginous flax-seed ooids with bioclastic, quartz (100 µm), or rare lithoclastic nuclei. The ooids are embedded in dolomite and ferruginous clayey matrix and cement (mineralogy is described here: doi:10.26302/SSHADE/EXPERIMENT_BS_20200813_100).

- Stratiform hematite vein and metasomatism in Oxfordian limestone (Pierremorte, south-east France). The ferruginized limestone contains ferruginized bioclast fragments in a partly ferruginized carbonated matrix (mineralogy is described here: doi:10.26302/SSHADE/EXPERIMENT_BS_20200815_100).

- Hettangian crinoidal limestone ferruginized by hydrothermal injection (Thoste, Burgundy, France). The limestone is partly replaced by iron oxides. It is composed mainly of entirely ferruginized crinoid fragments in a ferruginized carbonated cement (mineralogy is described here: https://doi.org/10.26302/SSHADE/EXPERIMENT_BS_20200812_100).

- Allochthonous bauxite trapped in a Middle Jurassic karst (Pierrerue Hérault, France). The reference samples are made of irregular ferruginous pisoliths coming from an iron duricrust in a bauxitic profile and containing mainly hematite and kaolinite (mineralogy is described here: doi.org/10.26302/SSHADE/EXPERIMENT_BS_20200814_100).

- Ferricrust from an ochre profile in the weathered Albian-Cenomanian glauconitic sand (Roussillon, Vaucluse, south-east France). Samples from the crust at the top of the ochre profile contain corroded quartz grains (200-400 µm) embedded with a kaolinitic and ferruginous matrix (mineralogy is described here: https://doi.org/10.26302/SSHADE/EXPERIMENT_BS_20191012_400).

- Fragments of ferruginous crust, remnants of a weathering profile developed on Urgonian limestone (Connaux, France) were used. This crust shows a lack of accessory minerals and a solely iron oxides and hydroxides content. REF. PIG rapport

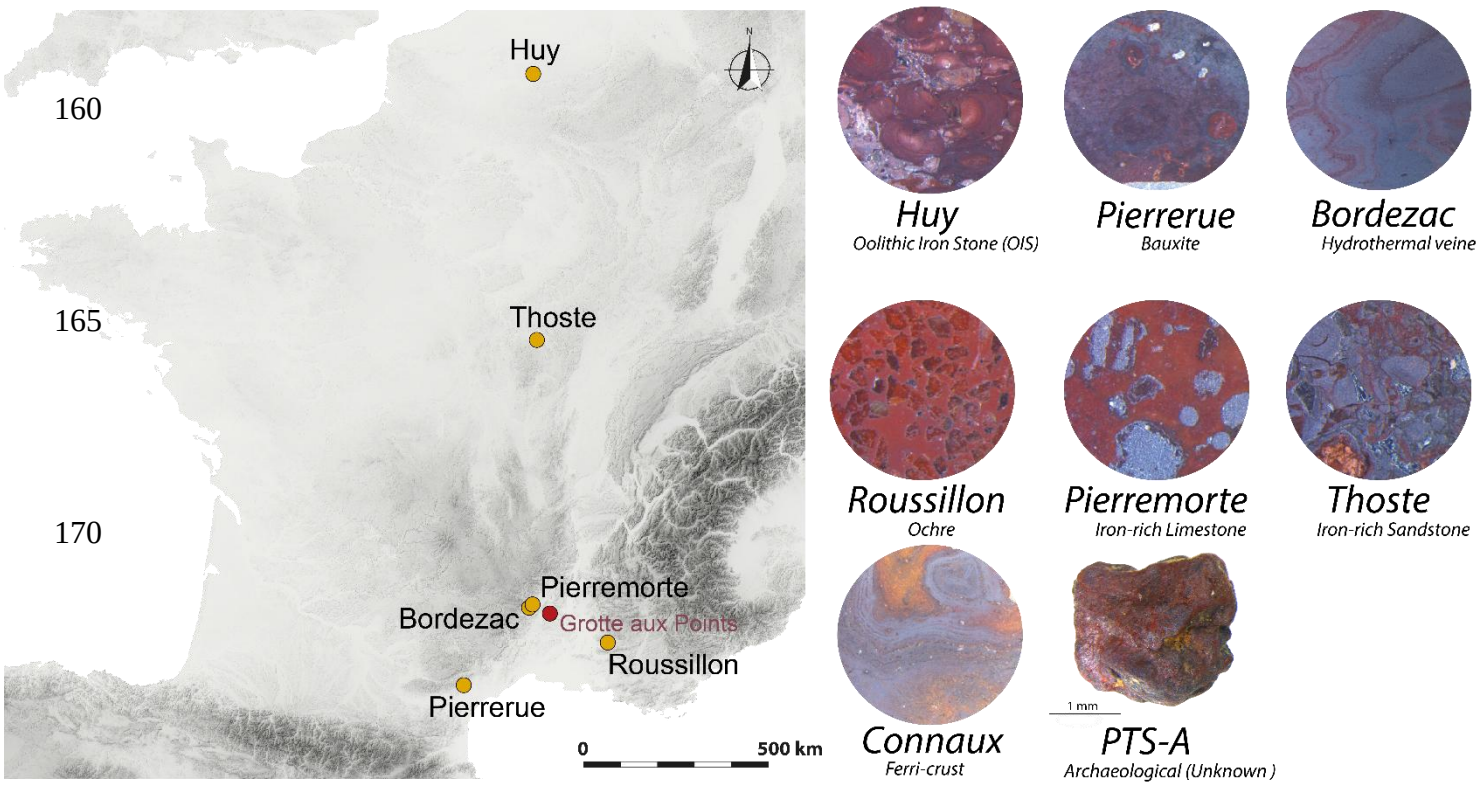

***Figure 02**: Localization map of the seven iron oxide-rich rocks used as references, associated to petrographic pictures on cross-sections*

To illustrate the method a set of data acquired on archeological colouring remains from the Grotte aux Points are used as a small "case study". These artefacts, coming from a Gravettian layer under the porch of the cave (Monney et al. 2018), measure between 2 and 5 mm in diameter. They show no trace of technical modification, including abrasion, scraping, heating or mixing with other minerals. However, they are certainly the remaining fragments of colouring powder production by crushing and grinding. From this corpus, the lithology A has been chosen for its well-known petrographic characteristics: iron oxide-rich clayish matrix (>60%) with green clayish inclusion: celadonite/glauconite, poor content in terrigenous detrital grains (quartz, heavy minerals rich in zirconium and titanium rich minerals) (Chanteraud et al. 2021, Chanteraud et al. 2019).

2.2. Sample preparation

The experimental dataset was generated by preparing polished cross-sections of geological references. This approach allowed for the identification of chemical variations associated with petrographic features and ensured the use of analytical conditions suitable for archaeological remains.

Rock samples were cut, embedded in an epoxy resin, sawed, and polished to a quarter micron (detailed protocol in Chalmin et al. 2021).

Archaeological items were not subject to a specific preparation such as cross-section, polishing and embedded. Only a surface of 400 µm x 400 µm was cleaned with a sterile scalpel blade to ensure that the burial sediment would not contaminate the analysis of the colouring material.

3. Method: PIXE analysis

3.1. Experimental conditions & parameters

For the µPIXE analyses AGLAE facility (C2RMF, Paris), we used a 30-µm extracted beam and filtered the signal by placing a 50-µm-thick aluminium film and a 13-µm chromium filter in front of the three high-energy detectors. As well as minimising the influence of Al, Si, Ca and Fe, these filters reduced pile-up effects caused by the high content of iron in the matrix, thereby improving the detection and quantification of trace elements. Detection limits are between 10 and more than 100 ppm according to the element. The analyses were performed under environmental condition (at air atmospheric pressure), with a helium flow to increase the detection performance and reduce the loss of signal for light elements (Z<26). The X, Y, Z motorized sample holder allowed us to realise mappings, with a minimal step size of 10 µm (Lebon et al. 2018, Mauran et al. 2022).

The various analytical constraints linked to the physics of the particles as well as the specificities of the device and set up (Cr filter) were considered in the choice of marker elements. The chromium and vanadium contents were exploited from the low-energy detection of the corresponding photons, to avoid the mask induced by the chromium filter on the high-energy detection. Particular attention was paid to the pile-up effect (stacking of X-ray photons on the detector), which can be observed in the spectra around 13 keV and is known for the very energetic Kα1 excitation line at 6.4 keV of iron, which creates a mask or a possibility of confusion with several K and L lines of other elements (Table 1). This stacking can result in false element recognition by the peak assignment software, which is particularly true for the Kβ1 line of bromine at 13.2 keV, the Kα1 of rubidium at 13.37 keV and Lβ of lead at 12.6 keV. This false positive can in turn generate quantification errors on the Kβ1 line of arsenic at 11.72 keV which can be confused with the Kα1 of bromine at 11.9 keV.

2015								
Dose counts	Acquisition Time	Map size µm	Map size pixel	Filters				
				LE0	HE1	HE2	HE3	HE4
500000	300 s	1000 x 1000	50 x 50	-	13 µm CR + 50 µm Al	RBS	13 µm CR + 50 µm Al	13 µm CR + 50 µm Al

2018								
Dose counts	Acquisition Time	Map size µm	Map size pixel	Filters				
				LE0	HE1	HE2	HE3	HE4
500000	480 s	500 x 500 or 1000 x 1000	25 x 25 or 50 x 50	-	13 µm CR + 50 µm Al	RBS	13 µm CR + 50 µm Al	13 µm CR + 50 µm Al

2019								
Dose counts	Acquisition Time	Map size µm	Map size pixel	Filters				
				LE0	HE1	HE2	HE3	HE4
500000	480 s	500 x 500 or 1000 x 1000	25 x 25 or 50 x 50	-	13 µm CR + 50 µm Al	RBS	13 µm CR + 50 µm Al	13 µm CR + 50 µm Al

**********Table 01**: Analytical parameters: dose, acquisition time, mapping size, used in the 2015, 2018 and 2019 analytical campaigns**********

3.2. Data processing

In order to compare the geochemical signatures of various geological ferruginous rocks and establish a usable geochemical reference for archaeological ferruginous artifacts (including rocks, powders, residues, and paintings), we conducted a comprehensive analysis of iron oxide-rich mineral phases within the rocks. As iron is a common element across different rock types and artifacts, it serves as a key focal point for our study.

To identify the geochemical signature of the pigmentaceous mineral phase carrying the iron element, we considered the specificities of the rocks, each composed of distinct mineral phases with unique geochemistry. Accordingly, we processed the acquired chemical maps while accounting for this heterogeneity.

Our approach aims to construct a statistical reference that accommodates the diversity and variability of the rocks. To achieve this, we focused on the geochemical maps of iron content in the seven reference samples.

Firstly, we employed iron concentration mapping, where colour variation ranging from red (indicating the highest iron concentration) to blue (indicating the lowest iron concentration) was utilized (see Figure 3a). To grasp the chemical variability within these rocks, composed of diverse mineralogical constituents, and to enable the recognition of distinct rocks based on real analysis, we applied threshold-based mapping according to iron content (count/pixel). Depending on the rock under analysis, we identified 2 to 3 areas corresponding to iron content levels under 30%, between 30% and 60%, and above 60% (as depicted in Figure 3b). Subsequently, we quantified the elemental content within each threshold. Each extracted quantification was then used to illustrate the chemical variability of each reference sample.

This process resulted in the individual processing of 51 chemical maps across the seven geological reference samples, yielding 97 spectra that express the chemical diversity of the references and their

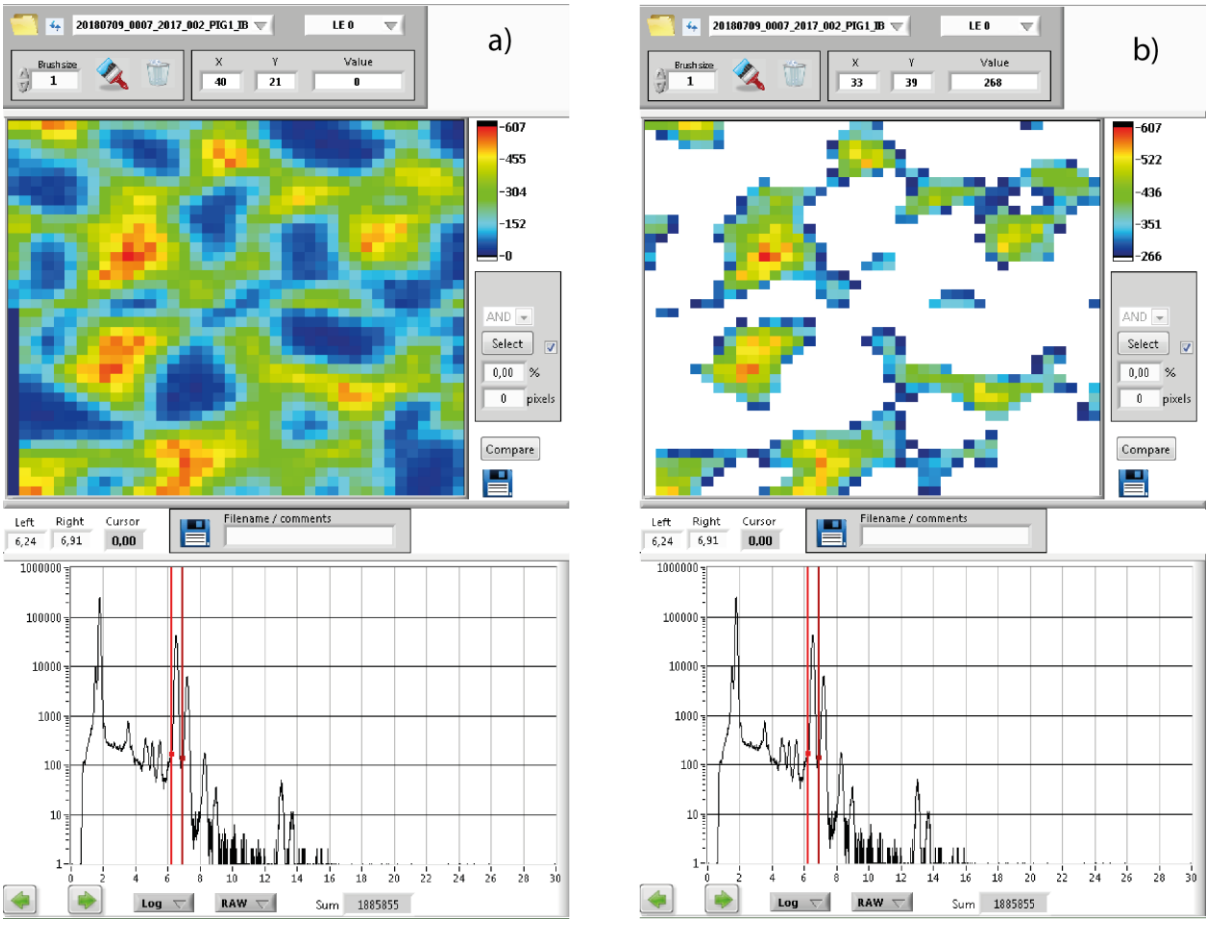

internal variability.

Figure 03**: iron content mapping on the "Roussillon" reference, a) observation of variation in iron content linked to different mineral phases (quartz, clay-iron matrix) by selecting iron peak on the spectrum, temperature colour scale expressed the iron content (count/pixel) and b) selection of pixels (20 x 20 µm) by thresholding the map above 400 counts/pixel (high iron content).************

The second step involved quantifying the elemental contents using GUPIXWIN (Campbell et al. 2021, 2010, 2000, 1995, 1989and TRAUPIXE software, applying the spectrum modelling and peak area calculation protocol as outlined by Pichon et al. (2010). Quantification in GUPIXWIN utilized a configuration file adapted from the works of Beck et al. (2012), Mathis et al. (2014) (Pichon et al. 2015).

As the third step, we applied a mathematical test to the quantification data to select measurements with an acceptable error, typically averaging less than 27%. This selection was based on a comparison between the calculated quantification and the fit error (calculated error) in relation to the detection limits (LOD). The threshold for data acceptability was determined using the following function:

$$If\ \frac{[elem] - \Delta[elem]}{100} < LOD[elem] = null(notmeasured)$$

[elem] is the calculated element concentration.

Δ [elem] is the incertainty in the calculation of the concentration.

LOD is the detection limit on the measurement

This sieving method retained only robust data suitable for chemical data analysis.

The fourth step involved the preparation of matrix data in tabular form. To identify specific finger-prints for each reference rock and to apply this method to archaeological artifacts, we focused on the signature related to iron content. In addition to the mapping threshold, we normalized the contents of major, minor, and trace elements by iron (in the form of ratios), followed by applying a base 10 logarithm to these ratios (*log ratio*, Aitchison, 1986).

Iron, being the common and sometimes major element in the analysed materials (often exceeding 70% concentration), can mask a significant portion of the information carried by other elements present in smaller quantities. Normalization by the iron content brings all elements to a comparable informative level, facilitating material differentiation even when elemental contents differ slightly (Popelka-Filcoff et al. 2008).

4. Study of the geochemical composition

4.1 Supervised statistical analysis by Linear Discriminant Analysis (ADL)

In the field of provenance research for archaeological materials, multivariate statistical tools play a pivotal role due to their capacity to process large volumes of data (Baxter, 1995, 2001, 2008; Aitchison, 1982). These tools operate by projecting the elemental content variables of each analyzed rock into a geometric space and measuring the distance between the chemical compositions of the compared references (Aitchison, 1982; Pearson, 1901).

Among the various statistical tools available, Linear Discriminant Analysis (LDA) stands out for its ability to predict the membership of a sample or archaeological artifact in a predefined group of references with known characteristics. LDA accomplishes this by leveraging the maximum difference (variance) between the data of each analyzed sample to construct a model that visually and mathematically distinguishes the references. Our choice to utilize LDA was driven by the need to assess its effectiveness in distinguishing well-known geological references through a comparison of their geochemical compositions. This approach aims to identify the key elements responsible for this distinction and the geological and mineralogical information they convey. Past 4.0 is employed for statistical analysis (Hammer et al., 2001).

4.1.1 Application of LDA on major and minor elements

Initially, we applied LDA to a selection of major elements known for their significance: Al, Si, Ca, K, and P. These elements were chosen because of their detectability and their association with major and minor mineral phases, rock types, and rock genesis. For instance, quartz is prevalent in continental or marine rocks, while calcite is characteristic of limestone and low-sea-level sedimentary rocks. Phyllosilicates like Al and Si are indicative of weathered minerals. This analysis of major and minor elements capitalizes on the expected robust signal provided by the host rock in which iron mineralization occurs. Additionally, this element selection minimizes the potential for contamination (e.g., Na, S, Cl) and focuses on elements consistently detectable, excluding those not systematically observed (e.g., Mg, Ti, Mn).

As a result of this approach, we were able to distinguish the Roussillon ochre from other geological samples due to the presence of quartz grains (Si) and kaolinite (Al silicate). The bauxite from Cazouls-lès-Béziers/Pierrerue stood out due to its high content of clay minerals with low alkaline and Al-hydroxide content. The ferruginized limestone from Pierremorte was well-defined by its elevated calcite content, while the oolithic hematite from Huy was characterized by its medium calcite content and the presence of illite and mica (Al, Si, and K). The Bordezac hematite mineralization exhibited a low content of mica (K, Al, Si) and quartz, distinguishing it from the other reference samples. Finally, the mineralized limestone from Thoste displayed contributions of calcite and K-rich silicates, although the exceedingly high iron content limited the differentiation of this set of measurements.

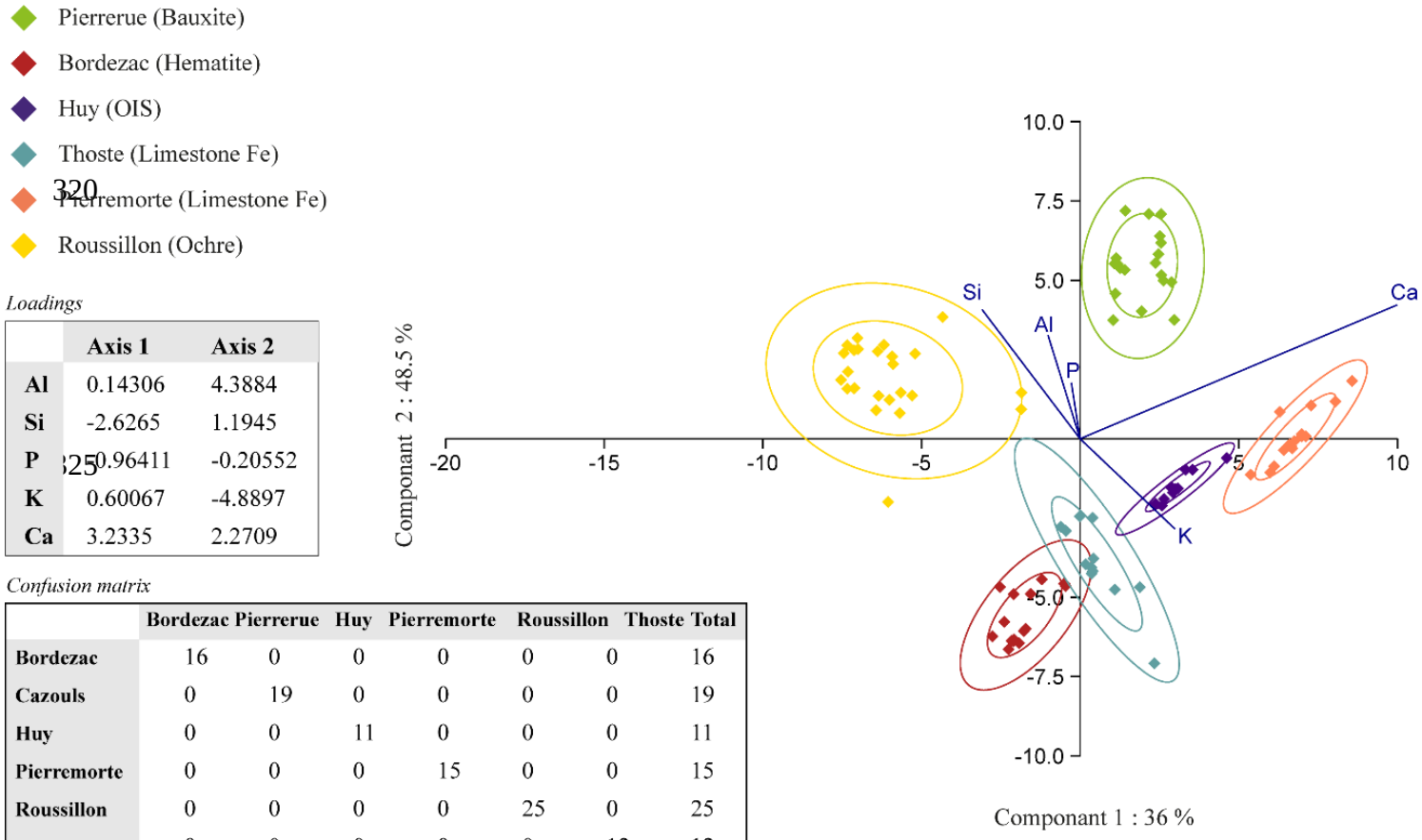

Loadings

	Axis 1	Axis 2
Al	0.14306	4.3884
Si	-2.6265	1.1945
P	0.96411	-0.20552
K	0.60067	-4.8897
Ca	3.2335	2.2709

Confusion matrix

	Bordezac	Pierrerue	Huy	Pierremorte	Roussillon	Thoste	Total
Bordezac	16	0	0	0	0	0	16
Cazouls	0	19	0	0	0	0	19
Huy	0	0	11	0	0	0	11
Pierremorte	0	0	0	15	0	0	15
Roussillon	0	0	0	0	25	0	25
Thoste	0	0	0	0	0	12	12
Total	16	19	11	15	25	12	98

***Figure 04**: LDA results on the set of compositional data of major and minor elements (normalised to iron concentration and log 10 transformed), that illustrate a geological signification. The ellipses (probabilistic space) are set at 95% (2 sigma) & 63% (1 sigma) and constructed from the uncertainty of the statistical calculations. The results explain 84% of the variance between the 6 geological references. The individual prediction (confusion matrix) is good: no misclassification.*

The graph and confusion matrix in Figure 4 demonstrate the profound influence of each rock's mineral composition on their geochemical characteristics. These chemical traits are shaped by various processes, including impregnation by mineralizing fluids from the host rock, such as in the cases of Pierremorte and Thoste limestones, or weathering of parent rocks, as observed in Roussillon's glauconitic sandstone (containing quartz and kaolinite) and Cazouls-lès-Béziers/Pierrerue bauxite (with Si and Al trapped in limestone depressions). Within this diverse family of rocks, minor elements like P and K exhibit differences corresponding to minor mineral phases, such as apatite in Thoste ferruginous limestone, illite and micas in Huy's oolithic ironstone (K), and micas in Bordezac (K).

Rocks containing iron oxide can be effectively discriminated based on major and selected minor elements. This result can be reached by observation at mesoscopic scale using petrographic charts of qualitative and quantitative descriptions (Cayeux 1929; Choquette and Pray, 1970; Deer et al., 2013; Dunham, 1962; Folk, 1951; Pettitjohn et al. 1987; Tucker & Wright (1990); Raymond, L. A., 1984, Petrography Laboratory Manual, vol. 1: Hand specimen Petrography. Geology Services International, NC, 170 p.; Terry and Chillingar (1955); Terry, R. D. and Chilingar, C. V. (1955) Summary of "Concerning some additional aids in studying sedimentary formations" by M. S. Shvetsov. Journal of Sedimentary Petrology, 25,229-214; In addition, major and minor elements like Si, Al, K, P, and Ca are often found in the sediments of archaeological sites and post-depositional concretions. As for pigments applied on walls and artefacts, these major elements belonging to the pigment and the support cannot be distinguished. The analysis has to be performed on fresh breaks or cleaned areas. Fur-

thermore, when two rocks originate from the same type of formation (e.g. two ferruginous limestones or ferricretes, etc.), the major elements may not be sufficiently discriminating to differentiate them (Mathis et al, 2014).

4.1.2 Application of LDA on trace elements

In order to avoid the influence of ubiquitous major elements, multivariate analysis was conducted (Figure 5) using four minor and trace elements related to iron content, which provided the best explanation of variance among the six references: V, Cr, Zn, and As. Discrimination was less efficient when using these minor and trace elements related to ferruginous minerals. Chromium and vanadium differentiated the Roussillon samples due to their high relative content in comparison to iron. Zinc was the key element distinguishing the bauxite samples, while arsenic was primarily associated with Thoste's hydrothermal hematite mineralization. Bordezac's hydrothermal deposit, impregnated limestone from Pierremorte, and oolithic hematite from Huy grouped together without strong chemical links to these selected elements.

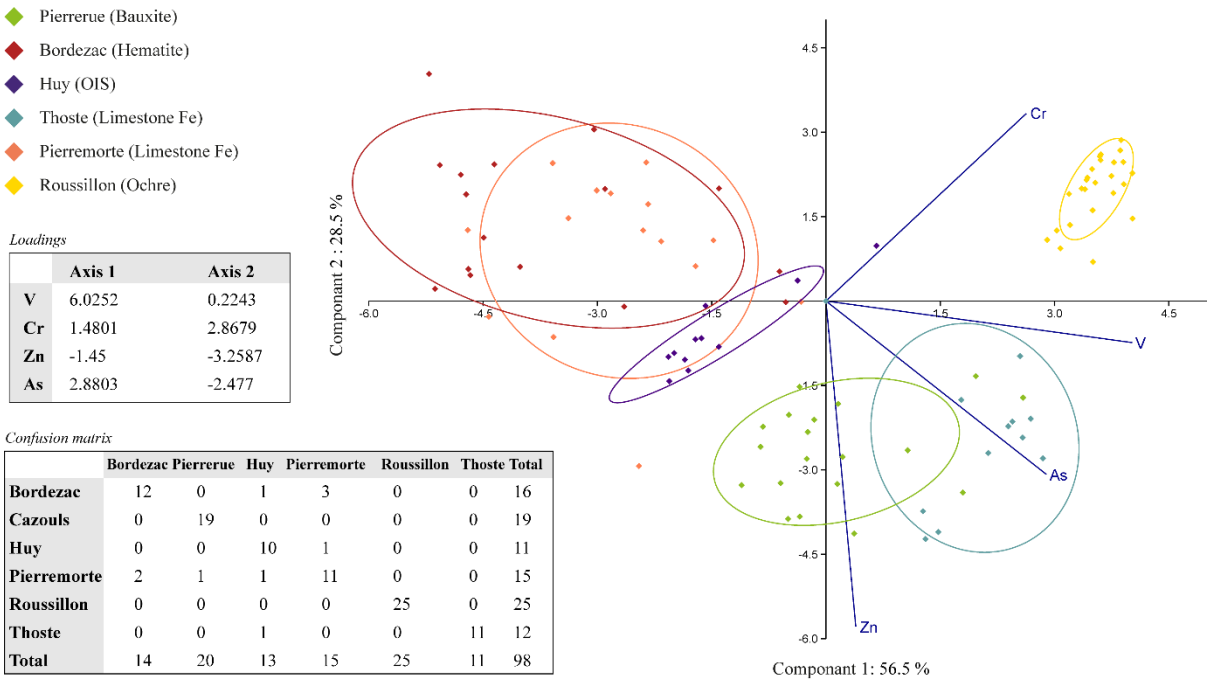

Loadings

	Axis 1	Axis 2
V	6.0252	0.2243
Cr	1.4801	2.8679
Zn	-1.45	-3.2587
As	2.8803	-2.477

Confusion matrix

	Bordezac	Pierrerue	Huy	Pierremorte	Roussillon	Thoste	Total
Bordezac	12	0	1	3	0	0	16
Cazouls	0	19	0	0	0	0	19
Huy	0	0	10	1	0	0	11
Pierremorte	2	1	1	11	0	0	15
Roussillon	0	0	0	0	25	0	25
Thoste	0	0	1	0	0	11	12
Total	14	20	13	15	25	11	98

***Figure 05**: LDA results on the set of compositional data of trace elements normalised to iron content and log 10 transformed, that can have a geological signification. For readability the ellipses (probabilistic space) are set at 63% (1 sigma) purpose and constructed from the uncertainty of the statistical calculations. The results explain 85% of the variance between the 6 references. The prediction of group membership is confused: 4 analysis points on the Bordezac hematite and one point on the Thoste ferruginous limestone are misclassified.*

4.1.3 LDA on trace element: Importance of reference selection

Among the six well-distinguished references, major elements carried the majority of the information, facilitating their differentiation from one another. In this case, trace elements were less informative and did not allow for differentiation as easily as major elements, particularly in the case of Bordezac

and Pierremorte, originating from the same hydrothermal region. Host rock and surrounding rock markers, such as Ca or Si, played a crucial role in differentiating them in the statistical analysis.

To emphasize the significance of carefully selecting references before conducting a statistical analysis, we introduced the Connaux reference into the discriminant analysis. Despite its high iron content, geographical origin, and genesis, Connaux reference exhibited geochemical similarities to other references in terms of major elements, such as Bordezac, Huy, and Thoste.

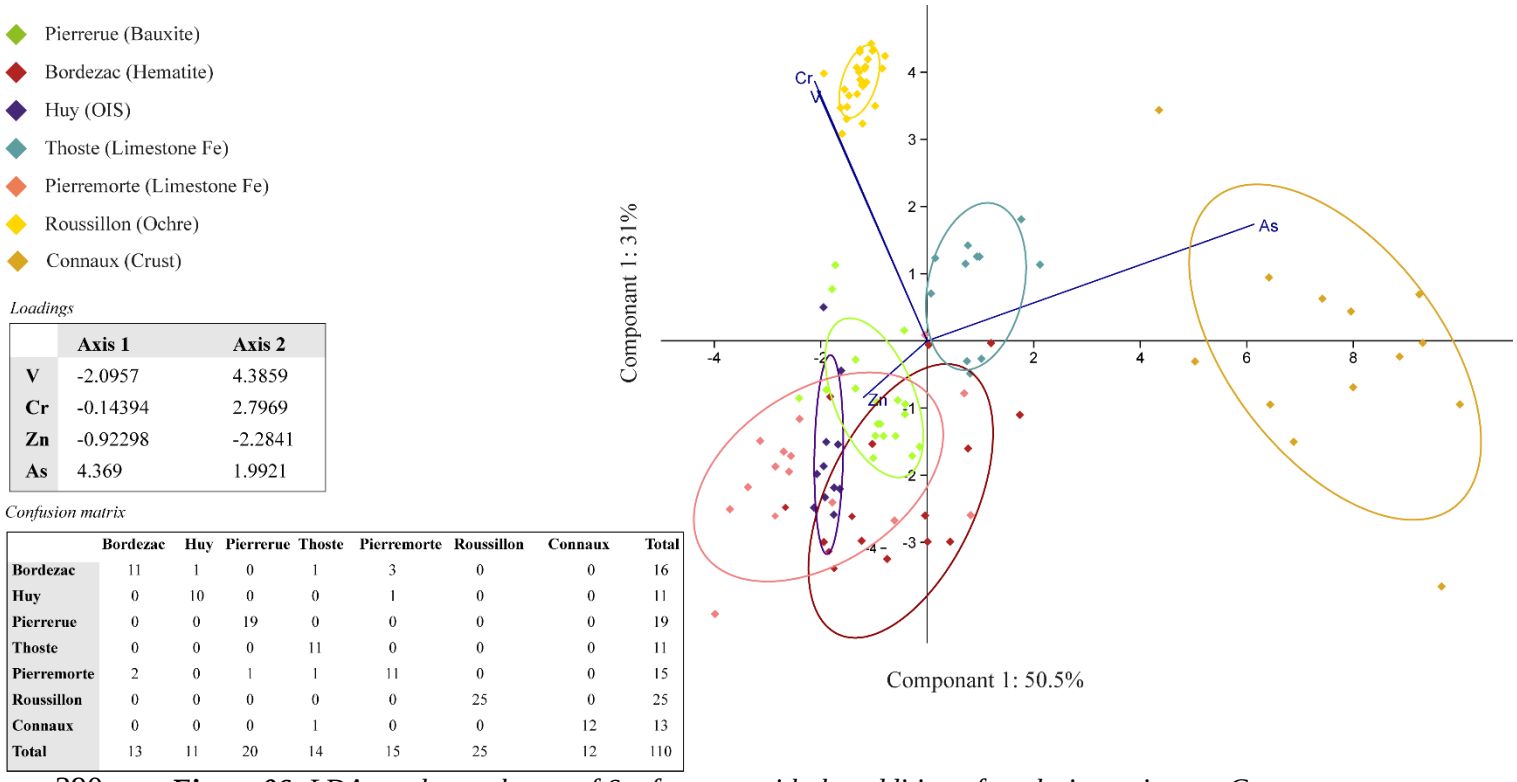

Loadings

	Axis 1	Axis 2
V	-2.0957	4.3859
Cr	-0.14394	2.7969
Zn	-0.92298	-2.2841
As	4.369	1.9921

Confusion matrix

	Bordezac	Huy	Pierrerue	Thoste	Pierremorte	Roussillon	Connaux	Total
Bordezac	11	1	0	1	3	0	0	16
Huy	0	10	0	0	1	0	0	11
Pierrerue	0	0	19	0	0	0	0	19
Thoste	0	0	0	11	0	0	0	11
Pierremorte	2	0	1	1	11	0	0	15
Roussillon	0	0	0	0	0	25	0	25
Connaux	0	0	0	1	0	0	12	13
Total	13	11	20	14	15	25	12	110

***Figure 06**: LDA results on the set of 6 references with the addition of analysing points on Connaux reference. For readability the ellipses (probabilistic space) are set at 63% (1 sigma) purpose and constructed from the uncertainty of the statistical calculations. The results explain 81.5% of the variance between the 7 references. The prediction of group membership is confused: 4 analysis points on the Bordezac hematite, 1 on Huy (OIS), 4 on Pierremorte (Limestone Fe) and one on Connaux are misclassified.*

In the case of trace elements, the introduction of Connaux's reference could be distinguished by its arsenic content. However, this elevated arsenic content grouped the other references (Bordezac, Pierrerue, Pierremorte, and Huy) with lower arsenic content, making them appear similar in the discriminant analysis (figure 6). Consequently, for a statistical analysis based on geochemical data from archaeological remains, the use of Connaux's reference may not be suitable if the arsenic content is not comparable.

4.2 Application on Grotte aux Points's colouring materials

Geological references Thoste and Huy are not used in the following statistical analysis because these are marine shallow sedimentary rocks, containing bioclasts and ooides, which are absent of the Grotte

aux Points artefacts. We rather concentrate on the regional references representing each category of rock.

In addition, Connaux was ruled out because of the high Arsenic content which is not comparable into the other references and archaeological artefacts.

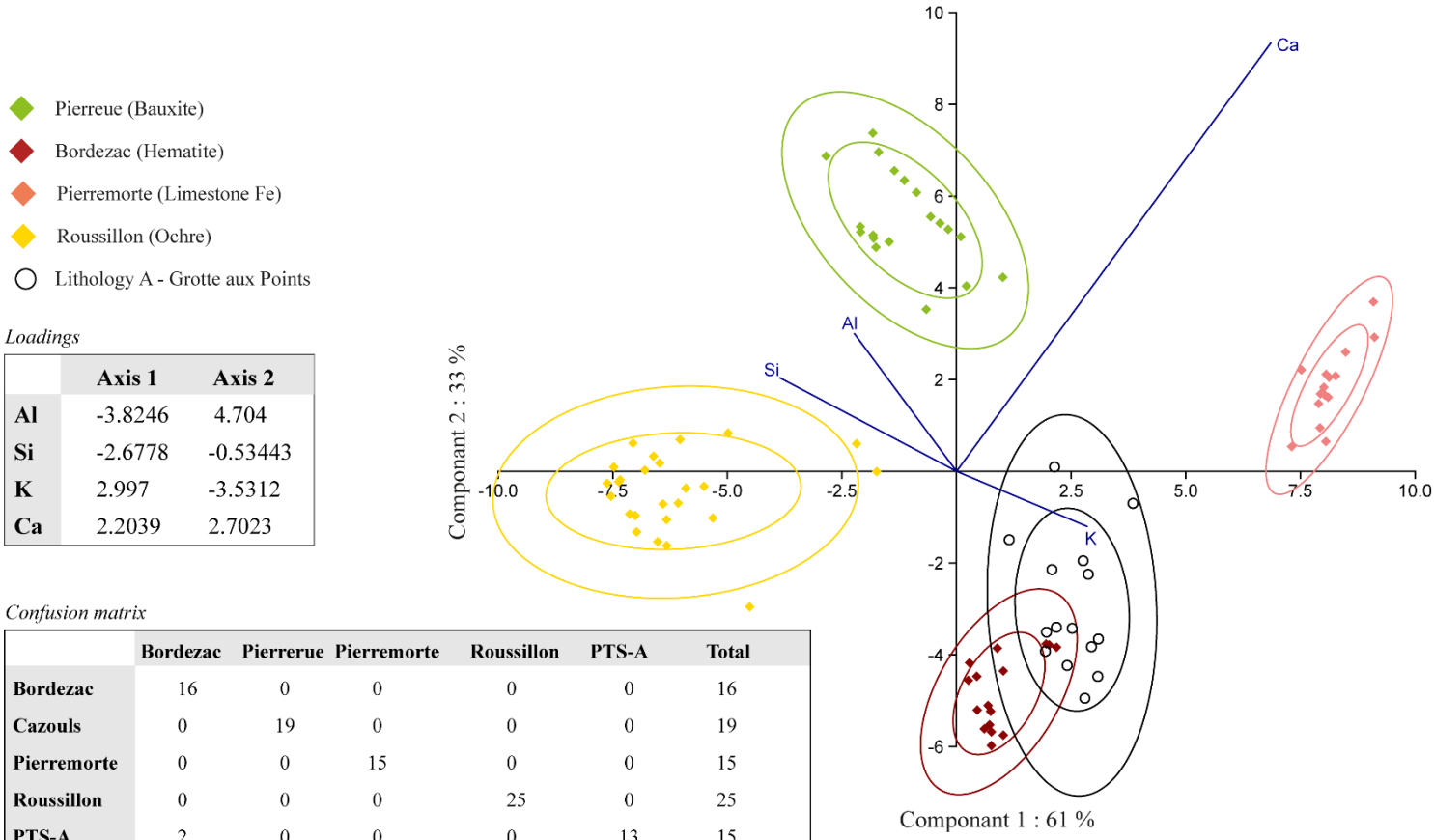

Loadings

	Axis 1	Axis 2
Al	-3.8246	4.704
Si	-2.6778	-0.53443
K	2.997	-3.5312
Ca	2.2039	2.7023

Confusion matrix

	Bordezac	Pierrerue	Pierremorte	Roussillon	PTS-A	Total
Bordezac	16	0	0	0	0	16
Cazouls	0	19	0	0	0	19
Pierremorte	0	0	15	0	0	15
Roussillon	0	0	0	25	0	25
PTS-A	2	0	0	0	13	15
Total	18	19	15	25	13	90

***Figure 07**: Integration test of a set points on raw colouring material from the Grotte aux Points (Lithology A) in the previous contrasted model. LDA was run on the set of major elements content log ratios calculated on 4 suitable references and the A lithology from the Grotte aux Points. The ellipses are set at 95% (2 sigma) & 63% (1 sigma). The results explain 94% of the variance between the 5 groups, and the prediction tend to put the A lithology in the Bodezac-hematite group.*

The patterns shown in Figure 7 tell that the lithology A of the Grotte aux Points shows proximity to the Bordezac reference materials based on the ratios of major element compositions to the iron that have the same range order. The presence of both quartz and K-phyllosilicates in Bordezac and lithology A also explain this proximity.

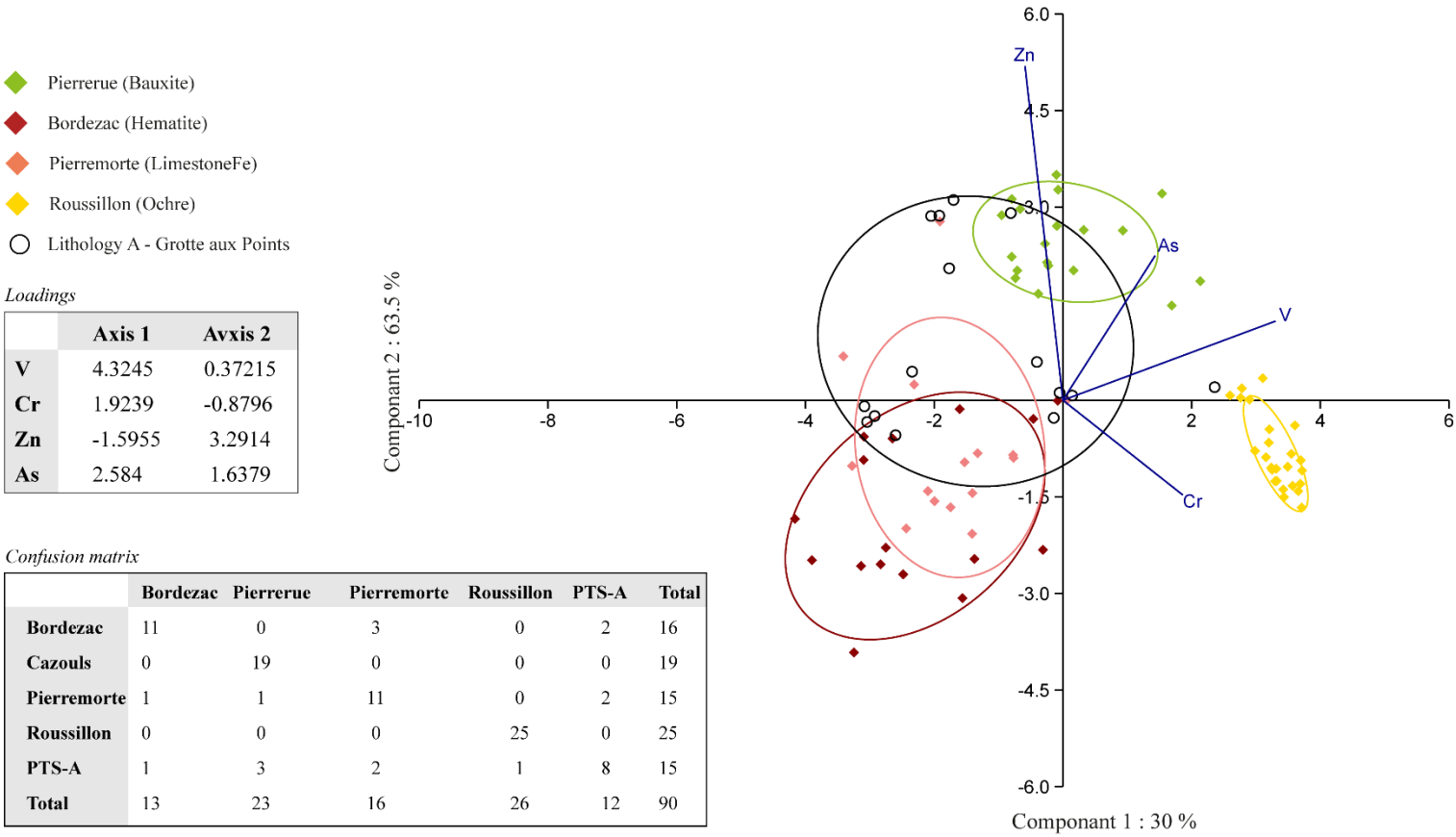

Loadings

	Axis 1	Avxis 2
V	4.3245	0.37215
Cr	1.9239	-0.8796
Zn	-1.5955	3.2914
As	2.584	1.6379

Confusion matrix

	Bordezac	Pierrerue	Pierremorte	Roussillon	PTS-A	Total
Bordezac	11	0	3	0	2	16
Cazouls	0	19	0	0	0	19
Pierremorte	1	1	11	0	2	15
Roussillon	0	0	0	25	0	25
PTS-A	1	3	2	1	8	15
Total	13	23	16	26	12	90

Figure 08: *Integration test of a set points on raw colouring material from the Grotte aux Points (Lithology A) in the previous constructed model. The model was reduced to 4 references in accordance with the A lithology specificities. The ellipses are set at 63% (1 sigma). The results explain 93.5% of the variance between the 5 groups, and the prediction tend to put the A lithology in the Bordezac-hematite group.*

The trace element compositions show a strong affinity to the data on the archaeological objects composed of hydrothermal hematite (Bordezac and Pierremorte). But, another subset of the data shows a remarkable affinity with the bauxite of Cazouls-lès-Béziers/Pierrerue. It is important to understand here that heterogeneity of the rock, carried by the different mineral phases, determines its geochemical signature. This demonstrates, despite the affinity of the hydrothermal hematite with the materials of the Grotte aux Points, that these geological deposits are not the source of raw materials. The source of the materials used at the Grotte aux Points must have similar compositional heterogeneity because it must contain the same mineral assemblage in similar proportions. By way of example, titanium used as an adjustment variable, in this case, can lead to a biased interpretation: that the archaeological colouring material corresponds to the hydrothermal hematites of the Gard. This element makes it possible to group together the data from Bordezac, Pierremorte and the Grotte aux Points and to separate it from the data of Pierrerue (Figure 9). However, titanium is present in Roussillon and Pierrerue in the form of detrital grains resisting to leaching (Ti and, Fe-Ti oxides) whose abundance is heterogeneous, whereas titanium content is correlated to iron content and very weakly represented in the three other rocks mentioned above, which groups them together just as artificially as the arsenic of Connaux brought together impregnated limestone and sandstone, oolitic hematite and bauxite.

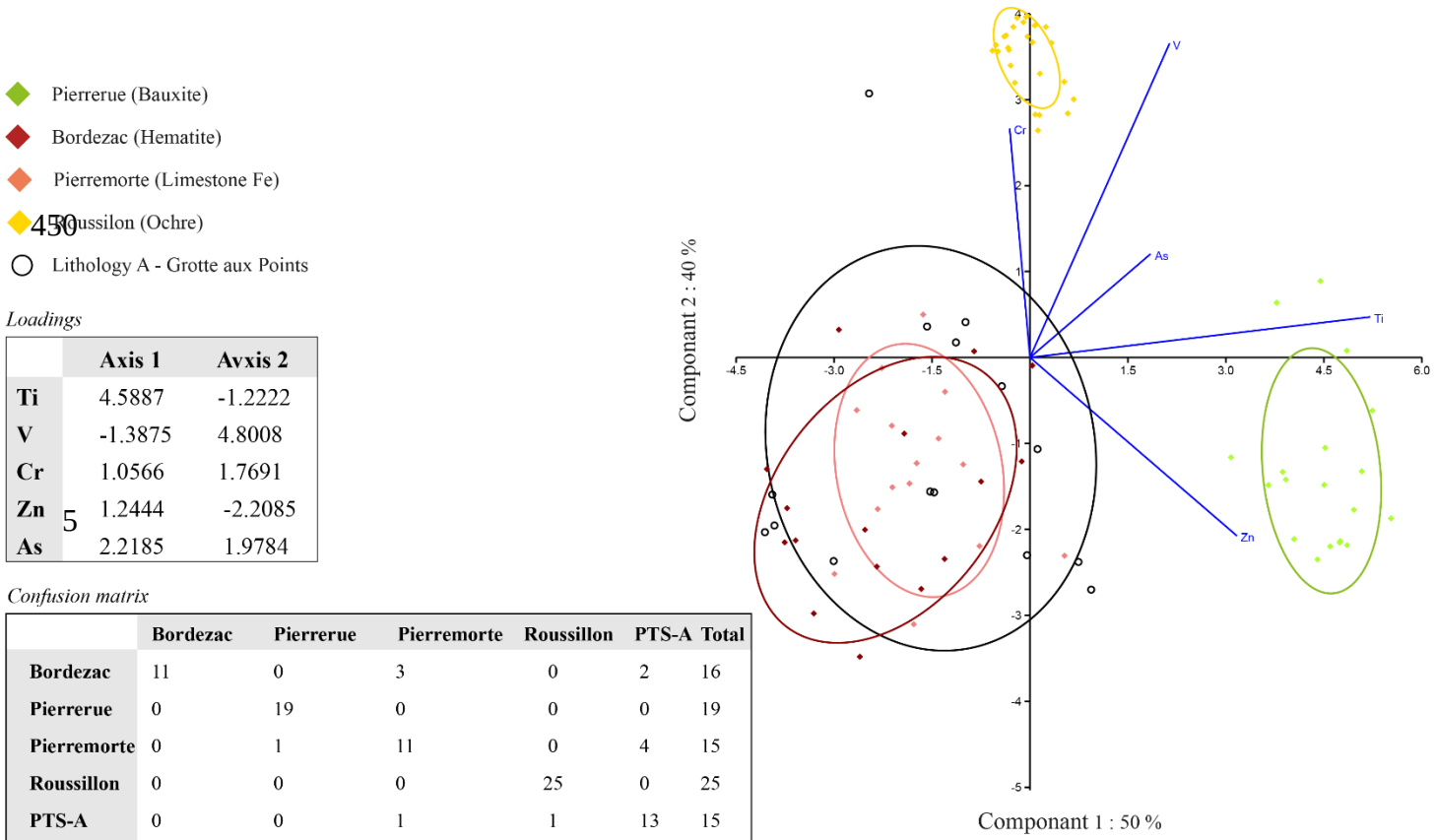

Loadings

	Axis 1	Avxis 2
Ti	4.5887	-1.2222
V	-1.3875	4.8008
Cr	1.0566	1.7691
Zn	1.2444	-2.2085
As	2.2185	1.9784

Confusion matrix

	Bordezac	Pierrerue	Pierremorte	Roussillon	PTS-A	Total
Bordezac	11	0	3	0	2	16
Pierrerue	0	19	0	0	0	19
Pierremorte	0	1	11	0	4	15
Roussillon	0	0	0	25	0	25
PTS-A	0	0	1	1	13	15
Total	11	19	15	26	19	90

***Figure 09**: Integration test of a set points on raw colouring material from the Grotte aux Points (Lithology A) in the previous contrasted model. LDA was run on the set of traces and minor (Ti added) elements content log ratios calculated on 4 suitable references and the A lithology from the Grotte aux Points. The ellipses are set at 95% (2 sigma) & 63% (1 sigma). The results explain 90% of the variance between the 5 groups, and the prediction tend to put the lithology A in the Bodezac-hematite group.*

5. Conclusion

Cohesive coloring materials are composed of mineral associations, each with its own physical and chemical properties. Consequently, a rock doesn't have just one, but multiple geochemical signatures corresponding to each mineral phase composing it. These various compositions, illustrating the mineral heterogeneity of the material, serve as evidence of the genesis of the rock and the natural or human history behind the coloring material found in archaeological sediments or on application supports like cave or shelter walls, bone or lithic industries, etc.

In addition to the question of the material's intrinsic heterogeneity, there's the inquiry into its history, whether natural or human-induced. Here, we refer to everything that can be added to the signal (petrography, mineralogy, and geochemistry) of the coloring material (cohesive or powder) after its deposition in a sedimentary sequence or as a powder or a mixture applied on a support.

A detailed and thorough description of the coloring material, its deposition context, and its human and natural history are essential to construct a meaningful geochemical analysis that corresponds to the reality of the material and its environment, regardless of its form and deposition mode.

Hence, without a comprehensive understanding of the petrography and mineralogy of the studied coloring materials, whether in cohesive or powder form (applied or not), conducting geochemical analyses is not reasonable. Microscope-based examination (optical and electron) allows for understanding mineral organization, describing geological formation modes, observing human and trans-

formation of the material, and comprehending the organization and interactions among applied coloring materials (powder), supports (walls, bones, flint, etc.).

This initial observational step generally helps determine major rock types (marine sedimentary, continental sedimentary, igneous, metamorphic, or volcanic) or morphologies and mineral associations (in the case of powders), facilitating initial comparisons. This visual identification of rock types also renders comparing major elements of geochemical composition unnecessary due to geological charts' availability for describing rocks.

Consequently, it becomes possible to select suitable mineral references (rocks) with similar characteristics for comparison with the studied archaeological objects and to build statistically relevant models considering the genesis, history, and evolution of the material.

These models are constructed step by step: based on trace element compositions (<1%) whose presence and origin can be understood and traced. Ubiquitous elements measurable in sediment, support, host rock, or any other mineral phase resulting from taphonomy are excluded. These elements must also fall within the detection limits of the device used and be adequately quantified (see detection limit).

Bridging the gap between applied powders and cohesive materials presents another challenge that cannot be addressed without this rigorous preliminary method, allowing an in-depth understanding of both the deposition and evolution conditions of the deposited material and the petrography of cohesive materials before constructing a comparative framework, avoiding false associations.

In conclusion, a comprehensive approach encompassing rock understanding, petrographic observation, archaeological observation (use/preparation), taphonomy, and a step-by-step approach to geochemistry consistent with observational elements is indispensable: without petrography, there's no geochemistry, so can we do without geochemistry?

We advocate the necessity to pose this question in a general context where scientific sobriety must prevail on the attraction generated by sophisticated cutting-edge technologies and complex statistical analysis. Therefore, in the study of coloring materials, petrographic observation (with and without preparation) aligns with both a robust and critical scientific approach as well as an ecological approach aiming to reduce research impacts on our environment, while enabling complex archaeological inquiries.

6. Data

S.I.1. Macroscopic pictures and SEM data and description of the Pigmentothèque references

Emilie Chalmin, Hélène Salomon, Aurélie Chassin de Kergommeaux, Claire Chanteraud. Construction d'une Pigmentothèque : un outil pour comprendre l'approvisionnement en matériaux colorants durant la Préhistoire. : Rapport d'activité 2019. [Rapport de recherche] DRAC/SRA; Auvergne Rhône Alpes. 2019. ⟨hal-02429867⟩

Emilie Chalmin, Hélène Salomon, Claire Chanteraud, Aurélie Chassin de Kergommeaux, B Schmitt, et al.. Constitution d'une "pigmentothèque" : un outil pour comprendre l'approvisionnement en matériaux colorants durant la Préhistoire : rapport intermédiaire 2020. [Rapport de recherche] DRAC/SRA Auvergne Rhône Alpes. 2021. ⟨hal-03161478⟩

Hélène Salomon, Emilie Chalmin, Claire Chanteraud, Aurélie Chassin de Kergommeaux, Marianne Le Turnier, et al.. Constitution d'une "Pigmentothèque" : un outil pour comprendre l'approvisionnement en matériaux colorants durant la Préhistoire. Rapport intermédiaire 2021. [Rapport de recherche] 2213729, DRAC - SRA Auvergne Rhône Alpes. 2022. ⟨hal-03539914⟩

Emilie Chalmin, Bernard Schmitt, Claire Chanteraud, Aurélie Chassin de Kergommeaux, Faycal Soufi, 2020. The contribution of diffuse reflectance spectroscopy to the knowledge of prehistoric red colouring matter, in: Proceedings of the AIC Interim Meeting Natural Colors-Digital Colors. Presented at the Natural Colors-Digital Colors, Avignon, p. 10.

S.I.2. PIXE data set

Chanteraud, Claire; Chalmin, Emilie (2019). pixe_rich_iron_standards_dataset. figshare. Dataset. https://doi.org/10.6084/m9.figshare.9798431.v2

S.I.3 AGLAE Map

Pichon, L., T. Calligaro, Q. Lemasson, B. Moignard, & C. Pacheco. (2015). "Programs for Visualization, Handling and Quantification of PIXE Maps at the AGLAE Facility." Nuclear Instruments and Methods in Physics Research Section B: Beam Interactions with Materials and Atoms, 363, 48-54. https://doi.org/10.1016/j.nimb.2015.08.086

https://sourceforge.net/projects/aglaemap/

S.I.4. Past - statistical analyses Software

Hammer, Ø., Harper, D.A.T., and P. D. Ryan, 2001. PAST: Paleontological Statistics Software Package for Education and Data Analysis. Palaeontologia Electronica 4(1): 9pp.

https://www.nhm.uio.no/english/research/resources/past/

https://www.nhm.uio.no/english/research/resources/past/downloads/past4manual.pdf

Acknowledgements

Reference and data collection was supported by the French department of Culture through a PCR granted by the Auvergne Rhône Alpes Regional Direction of Cultural Affairs (DRAC-ARA).This paper received support from AGLAE, the analytical PIXE platform dedicated to patrimony materials studies of the French Ministry of Culture. IPERION CH is a project funded by the European Commission, H2020-INFRAIA-2014-2015, under Grant No. 654028**.** Financial support was provided in part by National Science Foundation grant 2208558 awarded to the Archaeometry Laboratory at the University of Missouri Research Reactor. We acknowledge the use of the GPT-3.5-based AI language model developed by OpenAI. The AI model provided text editing, language assistance.

Bibliography

Aitchison, John. (1982). "The statistical analysis of compositional data." Journal of the Royal Statistical Society: Series B (Methodological), 44(2), 139-160.

Audouin-Rouzeau, F., & Plisson, H. (1982). "Les ocres et leurs témoins au Paléolithique en France: enquête et expériences sur leur validité archéologique." Cahiers du Centre de Recherches Préhistoriques, 8, 33-80.

Baxter, M. J. (1990). "Spatial k-means clustering in archaeology – variations on a theme."

Baxter, M. J. (1995). "Standardization and Transformation in Principal Component Analysis, with Applications to Archaeometry." Applied Statistics, 44(4), 513. https://doi.org/10.2307/2986142

Baxter, Michael J. (2001). "Statistical modelling of artefact compositional data." Archaeometry, 43(1), 131-147.

Baxter, MJ, CC Beardah, I Papageorgiou, MA Cau, PM Day, & V Kilikoglou. (2008). "On statistical approaches to the study of ceramic artefacts using geochemical and petrographic data." Archaeometry, 50(1), 142-157.

Beck, L, M Lebon, L Pichon, M Menu, L Chiotti, R Nespoulet, & P Paillet. (2011). "PIXE characterisation of prehistoric pigments from Abri Pataud (Dordogne, France)." X-Ray Spectrometry, 40(3), 219-223.

Beck, L., H. Salomon, S. Lahlil, M. Lebon, G.P. Odin, Y. Coquinot, & L. Pichon. (2012). "Non-Destructive Provenance Differentiation of Prehistoric Pigments by External PIXE." Nuclear Instruments and Methods in Physics Research Section B: Beam Interactions with Materials and Atoms, 273, 173-177. https://doi.org/10.1016/j.nimb.2011.07.068

Bellot-Gurlet, Ludovic, Gérard Poupeau, Joseph Salomon, Thomas Calligaro, Brice Moignard, Jean-Claude Dran, Jean-Alix Barrat, & Laurent Pichon. (2005). "Obsidian Provenance Studies in Archaeology: A Comparison between PIXE, ICP-AES and ICP-MS." Nuclear Instruments and Methods in Physics Research Section B: Beam Interactions with Materials and Atoms, 240(1-2), 583-588. https://doi.org/10.1016/j.nimb.2005.06.216

Billard, Cyrille, Xavier Savary, Dominique Bosquet, Ivan Jadin, Caroline Hamon, Éric Goemaere, Roland Dreesen, Lionel Dupret, & Guirec Querr. (2016). "Différenciation des hématites oolithiques à partir d'observations macroscopiques non destructives : essais de comparaison des matériaux ordoviciens normands et dévoniens belges." Anthropologica et Praehistorica, 125/2014, 193-202.

Calligaro, T., S. Colinart, J.-P. Poirot, & C. Sudres. (2002). "Combined External-Beam PIXE and μ-Raman Characterisation of Garnets Used in Merovingian Jewellery." Nuclear Instruments and Methods in Physics Research Section B: Beam Interactions with Materials and Atoms, 189(1-4), 320-327. https://doi.org/10.1016/S0168-583X(01)01078-3

Campbell, J.L., N.I. Boyd, N. Grassi, P. Bonnick, & J.A. Maxwell. (2010). "The Guelph PIXE Software Package IV." Nuclear Instruments and Methods in Physics Research Section B: Beam Interactions with Materials and Atoms, 268(20), 3356-3363. https://doi.org/10.1016/j.nimb.2010.07.012

Campbell, J.L., D.J.T. Cureatz, E.L. Flannigan, C.M. Heirwegh, J.A. Maxwell, J.L. Russell, & S.M. Taylor. (2021). "The Guelph PIXE Software Package V." Nuclear Instruments and Methods in Physics Research Section B: Beam Interactions with Materials and Atoms, 499, 77-88. https://doi.org/10.1016/j.nimb.2021.05.004

Chalmin, Emilie, & Jilian Huntley. (2017). "Characterizing Rock Art Pigments." In B. David & I. J. McNiven (Eds.), Oxford University Press.

Chanteraud, Claire. (2020). "Matières colorantes et grottes ornées des gorges de l'Ardèche. Méthodes d'analyse des ressources et liens culturels au Paléolithique supérieur : application à la grotte aux Points (Aiguèze, Gard, France)." Thèse, Université Savoie Mont Blanc. https://tel.archives-ouvertes.fr/tel-03184877

Chanteraud, Claire, Emilie Chalmin, S. Hoerlé, Hélène Salomon, & Julien Monney. (2019). "Relation entre les matières colorantes issues des fouilles et des parois ornées. Méthodologie et première perspective comparative à la Grotte aux Points (Aiguèze, Gard, France)." Karstologia, 73, 1-12. https://hal.archives-ouvertes.fr/hal-01756858

Chanteraud, Claire, Émilie Chalmin, Matthieu Lebon, Hélène Salomon, Kevin Jacq, Camille Noûs, Jean-Jacques Delannoy, & Julien Monney. (2021a). "Contribution and limits of portable X-ray fluorescence for studying Palaeolithic rock art: a case study at the Points cave (Aiguèze, Gard, France)." Journal of Archaeological Science: Reports, 37, 102898.

Chanteraud, Claire, Émilie Chalmin, Matthieu Lebon, Hélène Salomon, Kevin Jacq, Camille Noûs, Jean-Jacques Delannoy, & Julien Monney. (2021b). "Contribution and limits of portable X-ray fluorescence for studying Palaeolithic rock art: a case study at the Points cave (Aiguèze, Gard, France)." Journal of Archaeological Science: Reports, 37, 102898. https://doi.org/10.1016/j.jasrep.2021.102898

Terry, R. D. et Chilingar, C. V. (1955) Résumé de "Concerning some additional aids in studying sedimentary formations" par M. S. Shvetsov. Journal of Sedimentary Petrology, 25,229-214

David, B., E. Clayton, & A. L. Watchman. (1993). "Initial results of PIXE analysis on northern Australian ochres." Australian Archaeology, 36(1), 50-57.

David, Bruno, Eric Clayton, & Alan Watchman. (1993). "Initial results of PIXE analysis on northern Australian ochres." Australian Archaeology, 36(1), 50-57.

Dayet, Laure. (2021). "Invasive and Non-Invasive Analyses of Ochre and Iron-Based Pigment Raw Materials: A Methodological Perspective." Minerals, 11(2), 210. https://doi.org/10.3390/min11020210

Fernandes, Paul. (2012). "Itinéraires et transformations du silex : une pétroarchéologie refondée, application au Paléolithique moyen." PhD Thesis. http://www.theses.fr/2012BOR14533/document

Hammer, Ø., Harper, D.A.T., and P. D. Ryan, 2001. PAST: Paleontological Statistics Software Package for Education and Data Analysis. Palaeontologia Electronica 4(1): 9pp.

Lebon, M., L. Pichon, & L. Beck. (2018). "Enhanced identification of trace element fingerprint of prehistoric pigments by PIXE mapping." Nuclear Instruments and Methods in Physics Research Section B: Beam Interactions with Materials and Atoms, 417, 91-95. https://doi.org/10.1016/j.nimb.2017.10.010

Leroi-Gourhan, A. (1964). Le geste et la parole. Vol. 1. Albin Michel.

Lo Giudice, Alessandro, Debora Angelici, Alessandro Re, Gianluca Gariani, Alessandro Borghi, Silvia Calusi, Lorenzo Giuntini, et al. (2017). "Protocol for Lapis Lazuli Provenance Determination: Evidence for an Afghan Origin of the Stones Used for Ancient Carved Artefacts Kept at the Egyptian Museum of Florence (Italy)." Archaeological and Anthropological Sciences, 9(4), 637-651. https://doi.org/10.1007/s12520-016-0430-0

MacDonald, Brandi Lee, William Fox, Laure Dubreuil, Jazmin Beddard, & Alice Pidruczny. (2018). "Iron oxide geochemistry in the Great Lakes Region (North America): Implications for ochre provenance studies." Journal of Archaeological Science: Reports, 19, 476-490.

Mathis, F., O. Vrielynck, K. Laclavetine, G. Chêne, & D. Strivay. (2008). "Study of the Provenance of Belgian Merovingian Garnets by PIXE at IPNAS Cyclotron." Nuclear Instruments and Methods in Physics Research Section B: Beam Interactions with Materials and Atoms, 266(10), 2348-2352. [https://doi.org/10.1016/j.nimb.200

Mauran, Guilhem. (2019). "Apports méthodologiques à la caractérisation des matières colorantes : application à l'abri orné de Leopard Cave (Erongo, Namibie)." http://www.theses.fr/s216661.

Mauran, Guilhem, Matthieu Lebon, Florent Détroit, Benoît Caron, Alma Nankela, David Pleurdeau, & Jean-Jacques Bahain. (2019). "First in situ pXRF analyses of rock paintings in Erongo, Namibia: results, current limits, and prospects." Archaeological and Anthropological Sciences, 1-23.

Maxwell, J.A., W.J. Teesdale, & J.L. Campbell. (1995). "The Guelph PIXE Software Package II." Nuclear Instruments and Methods in Physics Research Section B: Beam Interactions with Materials and Atoms, 95(3), 407-421. https://doi.org/10.1016/0168-583X(94)00540-0

Menu, M, & Ph Walter. (1992). "Prehistoric cave painting PIXE analysis for the identification of paint "pots"." Nuclear Instruments and Methods in Physics Research B, 64, 547-552.

Monney, Julien. (2018). "La grotte aux Points d'Aiguèze, petite soeur de la grotte Chauvet, et les recherches menées dans le cadre du projet «Datation Grottes Ornées»." Karstologia, 72, 1-12.

Orange, Marie, François-Xavier Le Bourdonnec, Ludovic Bellot-Gurlet, Carlo Lugliè, Stéphan Dubernet, Céline Bressy-Leandri, Anja Scheffers, & Renaud Joannes-Boyau. (2017a). "On Sourcing Obsidian Assemblages from the Mediterranean Area: Analytical Strategies for Their Exhaustive Geochemical Characterisation." Journal of Archaeological Science: Reports, 12, 834-844. https://doi.org/10.1016/j.jasrep.2016.06.002

Orange, Marie, François-Xavier Le Bourdonnec, Ludovic Bellot-Gurlet, Carlo Lugliè, Stéphan Dubernet, Céline Bressy-Leandri, Anja Scheffers, & Renaud Joannes-Boyau. (2017b). "On Sourcing Obsidian Assemblages from the Mediterranean Area: Analytical Strategies for Their Exhaustive Geochemical Characterisation." Journal of Archaeological Science: Reports, 12, 834-844. https://doi.org/10.1016/j.jasrep.2016.06.002

Pearson, Karl. (1901). "Principal components analysis." The London, Edinburgh, and Dublin Philosophical Magazine and Journal of Science, 6(2), 559.

Pichon, L., T. Calligaro, Q. Lemasson, B. Moignard, & C. Pacheco. (2015). "Programs for Visualization, Handling and Quantification of PIXE Maps at the AGLAE Facility." Nuclear Instruments and Methods in Physics Research Section B: Beam Interactions with Materials and Atoms, 363, 48-54. https://doi.org/10.1016/j.nimb.2015.08.086

Querré, G., T. Calligaro, S. Domínguez-Bella, & S. Cassen. (2014). "PIXE Analyses over a Long Period: The Case of Neolithic Variscite Jewels from Western Europe (5th–3th Millennium BC)." Nuclear Instruments and Methods in Physics Research Section B: Beam Interactions with Materials and Atoms, 318, 149-156. https://doi.org/10.1016/j.nimb.2013.07.033

Querré, G, F Herbault, & Th Calligaro. (2008a). "Transport of Neolithic variscites demonstrated by PIXE analysis." X-Ray Spectrometry: An International Journal, 37(2), 116-120.

Querré, G., F. Herbault, & Th. Calligaro. (2008b). "Transport of Neolithic Variscites Demonstrated by PIXE Analysis." X-Ray Spectrometry, 37(2), 116-120. https://doi.org/10.1002/xrs.1031

Raymond, L. A., 1984, Petrography Laboratory Manual, vol. 1 : Hand specimen Petrography. Geology Services International, NC, 170 p.

Salomon, Hélène, Claire Chanteraud, Aurélie Chassin de Kergommeaux, Julien Monney, Jean-Victor Pradeau, Éric Goemaere, Yvan Coquinot, & Emilie Chalmin. (2021a). "A geological collection and methodology for tracing the provenance of Palaeolithic colouring materials." Journal of lithic studies, 8(1), 38-p. https://doi.org/10.2218/jls.5540

Salomon, Hélène, Claire Chanteraud, Aurélie Chassin de Kergommeaux, Julien Monney, Jean-Victor Pradeau, Éric Goemaere, Yvan Coquinot, & Emilie Chalmin. (2021b). "A geological collection and methodology for tracing the provenance of Palaeolithic colouring materials." Journal of lithic studies, 8(1), 38-p.